Chapter 14
E.COSY: Determination of Coupling Constants

Harald Schwalbe, P. Schmidt and Christian Griesinger

Institut für Organische Chemie, Johann Wolfgang Goethe-University, Max-von-Laue-Str. 7, 60438 Frankfurt, Germany

14.1 INTRODUCTION

Exclusive correlation spectroscopy (E.COSY)[1–3] is one of the most powerful methods for determining homonuclear, *J*(H,H) and *J*(C,C), as well as heteronuclear coupling constants, such as *J*(C,H), *J*(N,H), *J*(P,H), and *J*(P,C), in proteins and nucleic acids. Applications to other heteronuclear systems, especially in metalloorganic chemistry, have been successfully performed to measure, for example, metal–phosphorus, metal–carbon and metal–proton coupling constants. Due to the inherent features of the experiment, precise coupling constants can be determined even if the linewidth of the involved nuclei is large (macromolecules) or the coupling constant to be determined is small. This chapter presents the basic principle (see 14.2) and different experimental implementations (see 14.3–14.7) of the E.COSY experiment, together with examples. Relaxation effects that introduce systematic errors in the coupling constant determination will not be discussed here; the interested reader is referred to the literature cited.[4–8]

14.2 THE E.COSY PRINCIPLE

If in a three spin system consisting of spins ABC with nonvanishing couplings *J*(A,C) and *J*(B,C), A (in ω_1) is correlated with B (in ω_2) without mixing

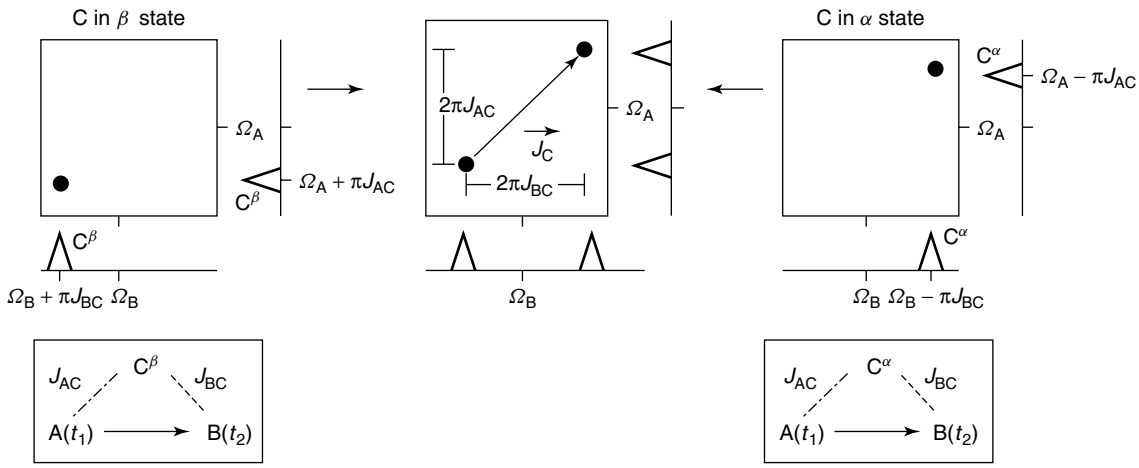

Figure 14.1. The E.COSY principle. In a three spin system the associated coupling J(A,C) is used to resolve the two components $\Omega_B \pm \pi J$(B,C) in ω_1. The two theoretical subspectra originate from spin C either in the α or in the β state.

the spin states of a third spin C (Figure 14.1), the two-dimensional correlation spectrum can be constructed from two subspectra with spin C either in the α or in the β state (Figure 14.1, left and right, respectively). Since spin A and spin B have a "chemical shift" of $\omega_1 = \Omega_A + \pi J$(A,C) and $\omega_2 = \Omega_B + \pi J$(B,C) for C in the α state, and of $\omega_1 = \Omega_A - \pi J$(A,C) and $\omega_2 = \Omega_B - \pi J$(B,C) for C in the β state, a spectrum that correlates spin A with spin B without touching C during t_1, the mixing, and t_2 will show just two cross peaks, one at $(\omega_1,\omega_2) = [\Omega_A + \pi J(A,C),\ \Omega_B + \pi J(B,C)]$ and the other at $(\omega_1,\omega_2) = [\Omega_A - \pi J(A,C),\ \Omega_B - \pi J(B,C)]$. The displacement vector $\boldsymbol{J}_C$ (where the subscript C indicates the passive spin in both dimensions) has the components J(A,C) and J(B,C) in ω_1 and ω_2, respectively. As can be derived from Figure 14.1, a small coupling J(B,C) can be determined, irrespective of its size, provided the so-called *associated coupling* J(A,C) is larger than the linewidth and the resolution in ω_1. The sensitivity of the experiment depends upon the transfer efficiency of the correlation between A and B, rather than on the size of the coupling of interest. The precision of the coupling constant determination depends on the precision with which the position of a peak maximum can be determined for a given digital resolution of the FID and digitization of the spectrum, and on the invariance of the submultiplets in the two slices displaced in ω_2. The direction of the displacement vector indicates the relative sign of the two couplings J(A,C) and J(B,C): it points to the upper right or lower left if the signs of the two couplings are the same; and it points to the upper left or lower right if the signs are different.

Depending on the spin systems under study (e.g. whether the molecule has the isotopes in natural abundance or the nuclei have been enriched with or depleted of the magnetically active isotope, the molecular weight of the compound under investigation, and the linewidth of the resonances), there are currently four different implementations of an E.COSY-type correlation (see 14.3–14.7). Rather than giving a chronological overview, the experiments are ordered according to their theoretical complexity. In the explanatory Figures given in each section, a representative pulse sequence, the spin system (with I_n, where I designates the ^{1}H spins, and n the numbers within them; S_n, where S designates the first heteronuclear spins, and n the numbers within them; and T for a second heteronuclear spin), the so-called E.COSY *triangle* and the resulting spectrum is shown. A dot in the spin system represents one or more non-NMR-active nuclei. The three essential spins A, B, and C are on the corners of the E.COSY triangle, the first active spin A (left) sharing a large, structurally uninteresting coupling with the passive spin C (top) which is used as an associated coupling to resolve the coupling of interest J(B,C) to spin B (right) which is the second active spin. In most of the proposed sequences, B is the detected spin. The sides of the triangle represent the associated coupling, the coupling of interest, and

the mixing process between A and B. A and B need not be directly scalar coupled. The E.COSY triangle may serve as a graphical aid in designing new experiments to measure coupling constants.

14.3 *S* FILTERED HOMONUCLEAR CORRELATION TO MEASURE $^nJ(I_2,S)$ COUPLINGS IN AN I_1–S–•–I_2 SPIN SYSTEM

In a three spin system I_1–S–•–I_2 with I_1 bound to S, the E.COSY pattern will be observed in any correlation between I_1 and I_2 obtained with an arbitrary homonuclear mixing sequence (e.g. TOCSY, NOESY, ROESY) because S remains untouched during the whole experiment (Figure 14.2(a)). S filtering can be inserted at the beginning of the pulse sequence to select for the NMR-active fraction of S nuclei. This classical Montelione–Wagner experiment[9,10] has been applied in a number of different applications for the measurement of J(C,H),[11–22] J(N,H),[23] J(P,H),[24] $J(^{113}$Cd,H),[25] J(F,H),[26] and J(F,C),[26] and is probably the best way to obtain coupling constant information for I_1–S–•–I_2 spin systems. It has been applied to the measurement of $^3J(\mathrm{N,H}_\beta)$, $^3J(\mathrm{N}_i,\mathrm{H}_{\alpha i-1})$, and ^3J(C,H) coupling constants. It fails, however, if the homonuclear mixing process is not efficient enough, as for example in α-helical regions of a protein where a NOESY transfer between $\mathrm{H}_i^{\mathrm{N}}$ and $\mathrm{H}_{\alpha i-1}$ is used for the measurement of the $^3J(\mathrm{N}_i,\mathrm{H}_{\alpha i-1})$ coupling constant, with N as the passive spin. The NOESY transfer between $\mathrm{H}_i^{\mathrm{N}}$ and $\mathrm{H}_{\alpha i-1}$ is insensitive in α-helical regions due to the large distance between these protons. In proteins, labeling of the heterospin S, especially that of ^{15}N, is indispensable for sensitivity reasons. Measuring long-range J(C,H) couplings with this approach in uniformly ^{13}C labeled proteins is difficult due to multiple carbon coupling partners. Selective decoupling schemes have been designed to avoid this problem.[27–32]

Figure 14.3 shows an application of the S filtered experiment.[18] The diastereotopic δ-methyl groups in leucines can be stereochemically assigned by measuring heteronuclear $^3J(\mathrm{C}_{\delta1},\mathrm{H}_{\beta1})$ and $^3J(\mathrm{C}_{\delta2},\mathrm{H}_{\beta1})$, or $^3J(\mathrm{C}_{\delta1},\mathrm{H}_{\beta2})$ and $^3J(\mathrm{C}_{\delta2},\mathrm{H}_{\beta2})$ couplings, respectively, provided the β-protons are stereochemically assigned. χ_2 of Leu_8 in cyclolinopeptide A assumes a position of 180°. This can be derived from the known stereochemical assignment $\mathrm{H}_{\beta1}$ = *pro-S* and $\mathrm{H}_{\beta2}$ = *pro-R*.

14.4 HETERONUCLEAR LONG-RANGE CORRELATION TO MEASURE $^nJ(I_1,I_2)$ COUPLINGS IN AN I_1–S–•–I_2 SPIN SYSTEM

Choosing I_2 (B) and S (A) as the two active spins and I_1 (C) as the passive spin, $^nJ(I_1,I_2)$ coupling constants can be measured provided I_1 is not touched between t_1 and detection. A heteronuclear multiple bond correlation (HMBC)-type sequence [Figure 14.2(b)][33] that correlates I_1 with S via the $^{n-1}J(I_1,S)$ coupling meets this requirement. The low efficiency of the mixing process due to the usually small heteronuclear $^{n-1}J(I_1,S)$ coupling and the short proton T_2 values are the limiting factors of the method.

14.5 THE SOFT-COSY EXPERIMENT TO MEASURE HOMONUCLEAR $^nJ(I_1,I_3)$ COUPLINGS IN AN I_1–I_2–I_2 SPIN SYSTEM AND HETERONUCLEAR $^nJ(S_2,I_1)$ COUPLINGS IN A S_2–S_1–•–I_1 SPIN SYSTEM

By application of selective pulses, a subset of spins of a certain isotope (e.g. H_α or C′) can be used as passive spins while using spins of another subset of the same isotope (e.g. H_β or C_α) as active spins. In proton correlation[34–37] spectroscopy [Figure 14.4(a)], this idea has not gained widespread application in peptide or protein spectroscopy, because there are no well separated subsets of proton spins that sustain at the same time interesting coupling constants. For example, in the case of $^3J(\mathrm{H}_\alpha,\mathrm{H}_\beta)$ coupling constants, when H_α is used as a passive spin and the two H_β are used as active spins the two subsets of passive and active spins are well separated; however, the associated coupling constant is a vicinal coupling, which can be very small. If, on the other hand, one of the H_β protons is used as a passive spin and the H_α and the other H_β proton as active spins, the associated coupling is a geminal coupling $^2J(\mathrm{H'}_\beta/\mathrm{H''}_\beta)$, but the spectral displacement between the two H_β protons is small.

For carbon, however, the spectrum is composed of well separated regions. Carbonyl and aliphatic carbon resonances have a large frequency difference compared with the chemical shift dispersion of aliphatic carbon atoms. Therefore selective pulses

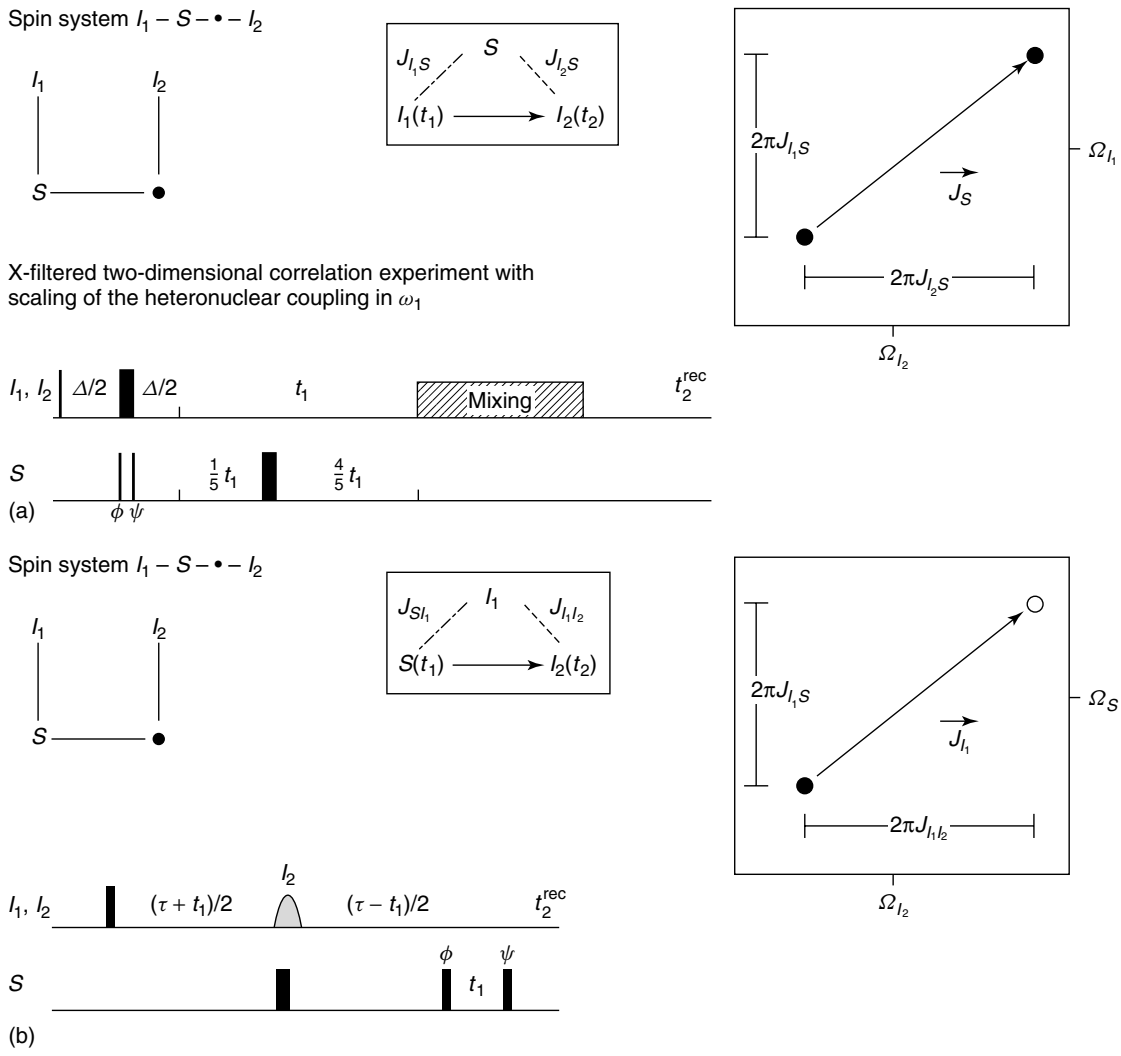

Figure 14.2. (a) The Montelione–Wagner experiment. In a heteronuclear I_1–S_1–•–I_2 spin system, I_1 and I_2 are correlated by an arbitrary homonuclear mixing process. The heterospin S is not touched and, therefore, remains passive during the entire experiment. Scaling of the associated coupling can be implemented to overcome problems due to overlap. The heteronuclear $^nJ(I_2,S)$ coupling is measured in t_2. The associated coupling $^1J(I_1,S)$ is scaled to 3/5 in t_1 in the example given. Typical parameters are: $\Delta = [J(I_1,S)]^{-1}$; $\phi = x, -x$; $\psi = x, x, -x, -x$; rec. $= x, -x, -x, x$. (b) The heteronuclear long-range experiment. In a heteronuclear I_1–S_1–•–I_2 spin system, S and I_2 are correlated; I_1 is untouched in the experiment. A homonuclear $^nJ(I_1,I_2)$ coupling is measured in t_2. The application of an I_2-selective refocusing pulse ensures pure phase lineshapes in t_2. The signal is modulated by long-range $^nJ(I,S)$ couplings in t_1 which are usually not resolved in t_1. Typical parameters are: $\tau \sim [2^{n-1}J(I_2,S)]^{-1}$; $\phi = x, -x$; $\psi = x, x, -x, -x$; rec. $= x, -x, -x, x$.

like the Gaussian cascades G3 and G4[38,39] or IBURP and REBURP pulses[40] effectively excite, for example, an aliphatic carbon spin S_1 while leaving the carbonyl spin S_2 passive. The $^1J(C',C_\alpha)$ coupling is, fortunately, large in proteins and can therefore be used as an associated coupling to measure $^2J(C',H_\alpha)$ in SOFT-HSQC,[41] or the structurally important $^3J(C',H_\beta)$ couplings in SOFT-HCCH-COSY[27]

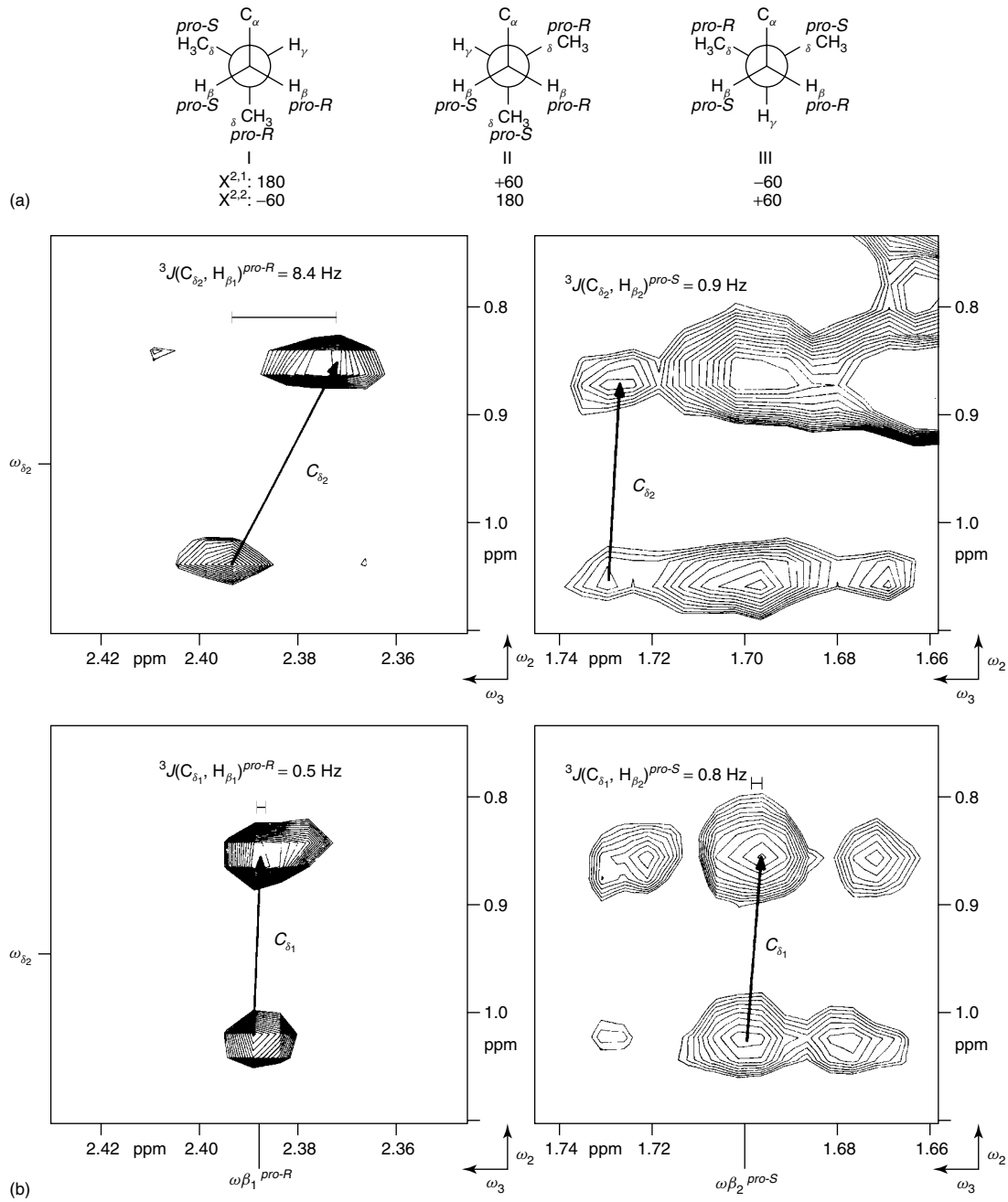

Figure 14.3. (a) Staggered rotamers around the C_β–C_γ bond of leucine. (b) Slices through the three-dimensional HSQC-TOCSY showing the four C_δ,H_δ,H_β cross peaks with the displacement vectors due to C_δ. The lower traces are taken at $\omega_1 = \delta(C_{\delta 1}) = 23.6$ ppm and the two upper traces at $\omega_1 = \delta(C_{\delta 2}) = 20.2$ ppm.

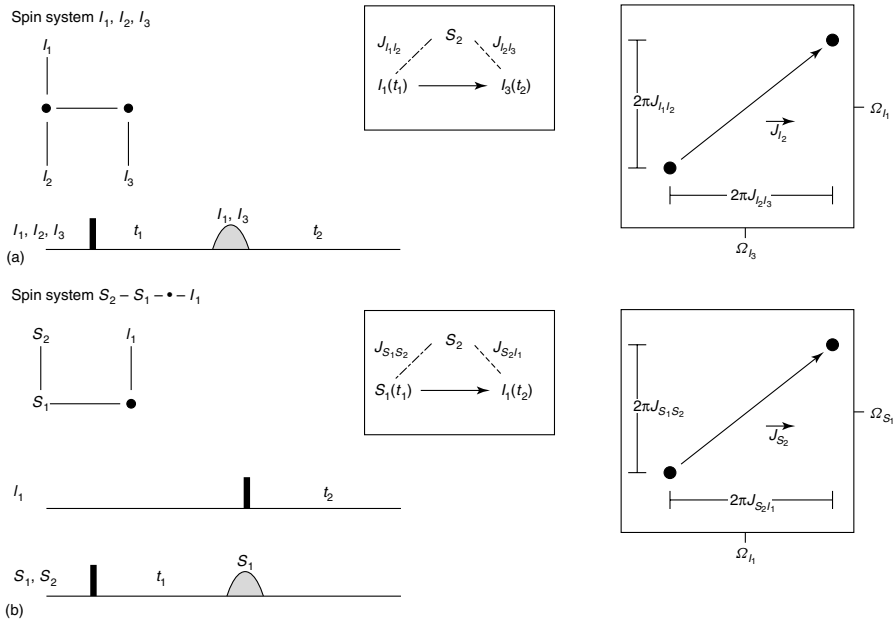

Figure 14.4. (a) The SOFT-COSY experiment. In a homonuclear three spin system, I_1 and I_3 are correlated by an I_1,I_3-selective mixing pulse. In the example given, the geminal $^2J(I_1,I_2)$ coupling is used as associated coupling in t_1. (b) The SOFT-hetero-COSY experiment. In the heteronuclear $S_2-S_1-\bullet-I_2$ spin system S_1-selective pulses leave the S_2 spin untouched. The homonuclear $^1J(S_1,S_2)$ coupling serves as an associated coupling in t_1.

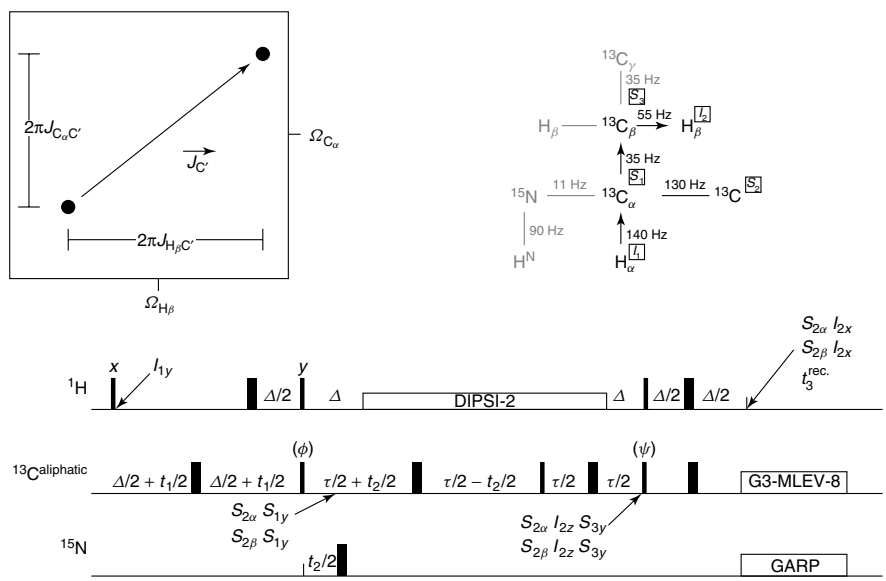

Figure 14.5. Pulse sequence for the SOFT-HCCH-COSY experiment. In the application to proteins, typical parameters are: $\Delta = [2^1J(C_\alpha,H_\alpha)]^{-1}$; $\tau = [2^1J(C_\alpha,C_\beta)]^{-1}$; $\tau' = [4^1J(C_\alpha,C_\beta)]^{-1}$; $\Delta' = [4^1J(C_\beta,H_\beta)]^{-1}$; $\phi = x, -x$; $\psi = x, x, -x, -x$; rec. $= x, -x, -x, x$.

(Figure 14.5) and the $^3J(C',H^N)$ couplings in the SOFT-HNCA-COSY.[42,43] A heteronuclear detected experiment for the opposite situation, in which S_1 and S_2 are protons, and I is a heteronucleus, has been published by Kessler *et al*.[44]

Figure 14.5 and Figure 14.6 show the application of this concept to measure $^3J(C',H_\beta)$ couplings in proteins. The constituent experiment is a SOFT-HCCH-COSY, in which $C_\alpha(A)$ is correlated with $H_\beta(B)$. In the constant time period $\tau = [2J(C_\alpha,C_\beta)]^{-1}$, the $^1J(C',C_\alpha)$ coupling, used as the associated coupling in t_1, has evolved a phase of 142°. Mirror image linear prediction[27,45,46] has to be applied to enhance the resolution in ω_1. From inspection of the $^3J(C',H_\beta)$ and the $^3J(H_\alpha,H_\beta)$ couplings (see 14.5) the conformation around χ_1 and the stereochemical assignments of the H_β protons can be derived. Four representative C_α,H_β cross peaks of the SOFT-HCCH-COSY and the SOFT-HCCH-E.COSY experiments (discussed in 14.6) measured on ribonuclease T_1 are shown. In each case, the unique pattern of large and small couplings provide the assignment to one of the three staggered rotamers. As shown in Figure 14.6, the predominant rotamer around χ_1 is $\chi_1 = -60°$ for Asn_{98}, since both $^3J(C',H_\beta)$ couplings are small and one $^3J(H_\alpha,H_\beta)$ coupling

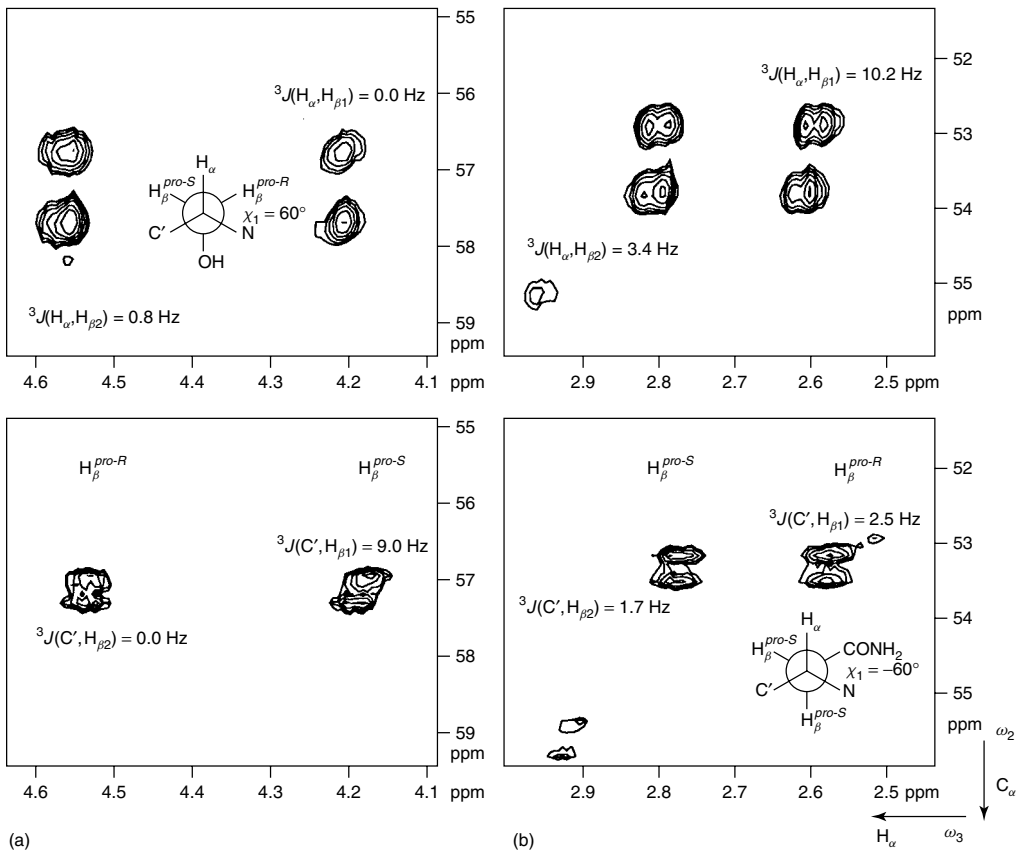

Figure 14.6. Cross peaks for: (a) Ser_{12}; (b) Asn_{98}; (c) Thr_{18}; (d) Ala_{21}. Upper and lower traces show the C_α,H_β cross peaks from the SOFT-HCCH-E.COSY and the SOFT-HCCH-COSY experiments, respectively. (a) Ser_{12} has two small $^3J(H_\alpha,H_\beta)$ couplings and one large $^3J(H_\beta,C')$ coupling. The predominant rotamer around χ_1 is therefore when $\chi_1 = 60°$, and the higher frequency $H_{\beta 1}$ is $H_\beta{}^{pro\text{-}R}$. (b) From the two small $^3J(H_\beta,C')$ couplings and the large $^3J(H_\alpha,H_{\beta 1})$ coupling of Asn_{98}, it follows that the predominant rotamer is at $\chi_1 = -60°$ and the higher frequency $H_{\beta 1}$ is $H_\beta{}^{pro\text{-}S}$. (c) Thr_{18} has a large $^3J(H_\alpha,H_{\beta 1})$ coupling of 9.3 Hz and a small $^3J(C',H_\beta)$ coupling of 3.0 Hz; χ_1 is therefore $-60°$. (d) The two cross peaks of Ala_{21} exhibit average $^3J(H_\alpha,H_{\beta 1})$ and $^3J(C',H_\beta)$ coupling constants of 6.8 and 4.2 Hz, respectively.

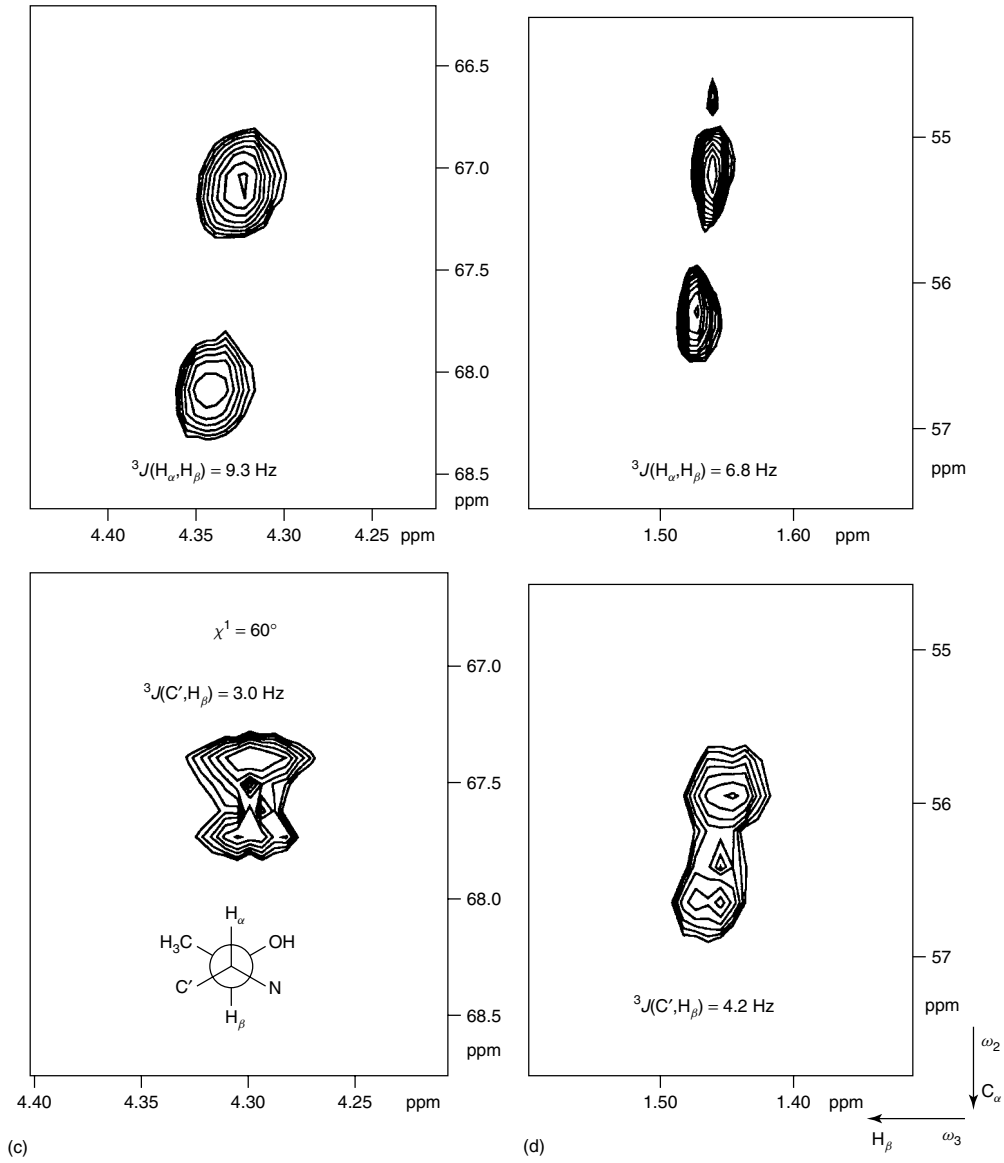

Figure 14.6. *Continued.*

is large. The lower frequency H_β can be assigned as *pro-R* since it shows a large coupling with H_α. The preferred conformation and the stereochemical assignment of the other residues are indicated on the figure.

Using the same basic experiment, homonuclear $^3J(C',C_\gamma)$ couplings can be determined for the stereochemical assignment of valine methyl groups in the SOFT-HCCC-COSY experiments[47] by correlating C_α (A) and C_γ (B), and leaving C' as the passive spin C. Figure 14.7 shows the pulse sequence for the SOFT-HCCC-COSY experiment, and Figure 14.8 shows the two C_α,C_γ cross peaks for Val_{16} in ribonuclease T_1. The large $^3J(H_\alpha,H_\beta)$ coupling of 12.4 ± 0.9 Hz and the small $^3J(C',H_\beta)$ coupling of 0.53 ± 0.4 Hz indicate a $\chi_1 = 180^\circ$ (not shown). Thus

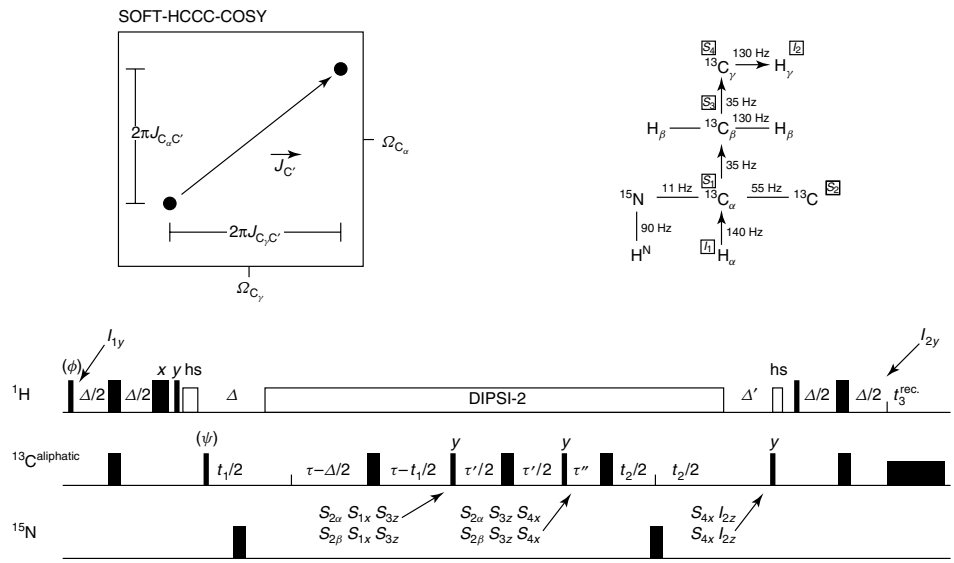

Figure 14.7. Pulse sequence for the SOFT-HCCC-COSY experiment. In the $S_2{-}S_1{-}\bullet{-}S_4$ spin system S_1,S_4 selective pulses leave S_2 untouched. The coupling of interest is measured in the ω_1,ω_2 cross peak of the three-dimensional experiment. In the application to proteins, typical parameters are: $\Delta = [2^1J(C_\alpha,H_\alpha)]^{-1}$; $\tau = [2^1J(C_\alpha,C_\beta)]^{-1}$; $\tau' = [(54/90)^1J(C,C)]^{-1}$; $\Delta' = [6^1J(C_\gamma,H_\gamma)]^{-1}$; $\phi = x, -x$; $\psi = x, x, -x, -x$; rec. $= x, -x, -x, x\tau'' \Delta^1 + t_2(0) + \tau_p$.

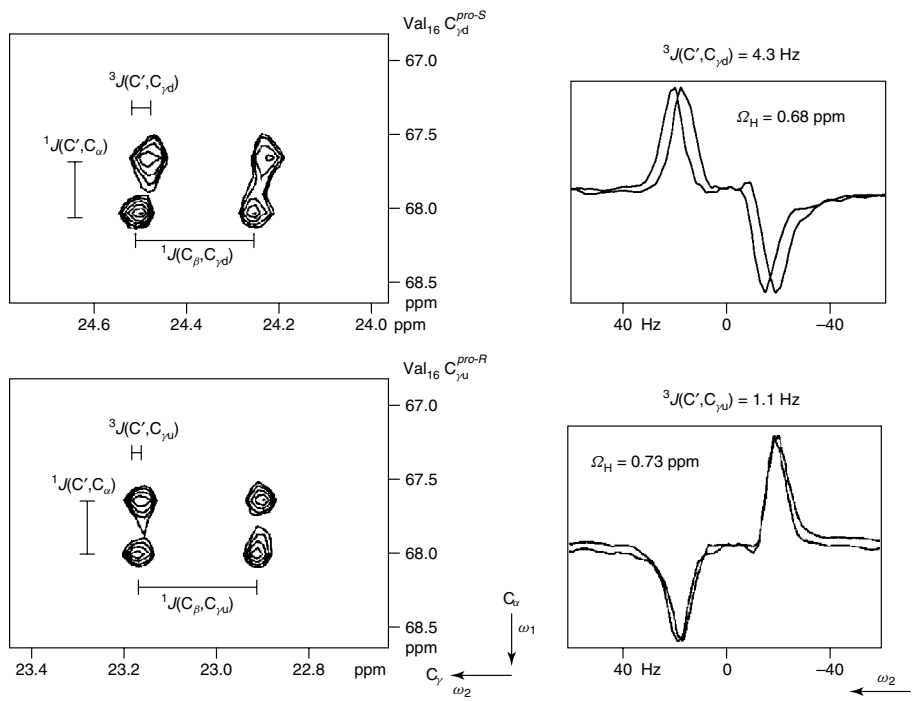

Figure 14.8. One-dimensional rows and two-dimensional slices from the SOFT HCCC-COSY on ribonuclease T_1. The C_β,H_β cross peaks are displaced due to C′. The antiphase splitting observed is the $^1J(C_\beta,C_\gamma)$ coupling of around 37 Hz.

the low-frequency C_γ is the *pro-R* carbon atom, and the high-frequency C_γ is the *pro-S* carbon atom.

14.6 BIRD PULSES FOR SPIN TOPOLOGY FILTERING: MEASURING HOMONUCLEAR $^nJ(I_1,I_2)$ COUPLINGS IN AN I_1–S–T–I_2 or I_1–S–•–I_2 SPIN SYSTEM

If one of the active spins (e.g. B) and the passive spin C have the same spin isotope (e.g. *I*) nonselective pulses cannot be used for polarization transfer from A to B, because C would be touched. However, spin topology filtering using the different transformation properties of two spins of the same isotope that are bound to different heteronuclei (e.g. $^1H-^{13}C$ and $^1H-^{15}N$) under bilinear rotation[48,49] can be used such that B is sensitive for the *I* pulses and C is not. Effective polarization transfer to B leaving C untouched is then possible. In the following, the different transformation properties of the I_2 spin (e.g. H_α) bound to the heteronucleus *S* ($^{13}C_\alpha$) and the I_1 spin (e.g. H^N) bound to *T* (^{15}N) under the BIRD sequence shown in Figure 14.9(a) will be discussed. Using the pulse scheme

$$90^\circ_x(I) - \Delta/2 - 180^\circ_y(I,T) - \Delta/2 - 90^\circ_{-x}(I) \tag{14.1}$$

a $2I_{1z}T_z$ operator that can be prepared after the evolution period of an HSQC-type experiment is transferred to detectable proton magnetization I_{1x}, whereas for spin I_2 which is not coupled to spin *T* the pulses can be concatenated to a $0^\circ(I)$ pulse. Thus I_2 is not affected during the polarization transfer from spin *T* to I_1.[42,43,50,51]

This principle has been applied in SOFT-HNCA-E.COSY experiments correlating $^{13}C_\alpha$ (A) with H^N (B). H_α is the passive spin C. N,H^N antiphase coherence is transferred to H^N magnetization without touching H_α. From this experiment $^3J(H^N,H_\alpha)$ couplings defining the backbone angle ϕ become available.[42,43,49–54] The BIRD-filtering concept is also compatible with the use of gradient sensitivity enhanced correlation,[42] yielding excellent water suppression and optimal sensitivity. Figure 14.10 shows the pulse sequences SOFT-HNCA-E.COSY

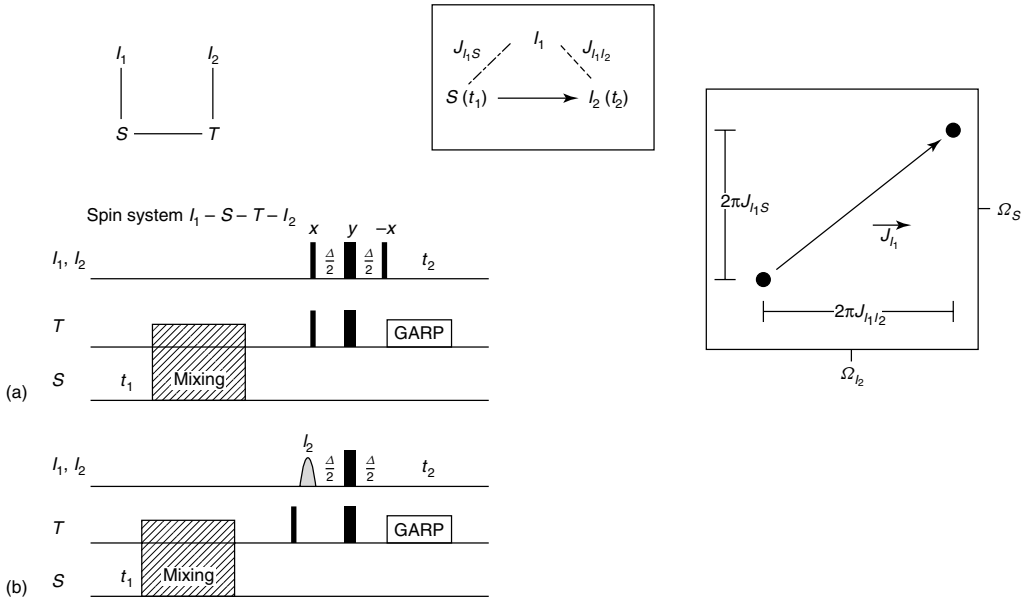

Figure 14.9. (a) Selection between homonuclear spins bound to different heterospins with BIRD pulses. In the I_1–S–T–I_2 spin system, I_2 bound to *T* evolves heteronuclear $J(I_2,T)$ coupling in the final BIRD refocusing period, whereas the spin states of I_1 bound to *S* remain unaltered. I_1 serves as passive spin, the $^nJ(I_1,I_2)$ coupling can be measured. For typical parameters see Figure 14.10. (b) Instead of using BIRD spin-topology-filtering techniques, I_2-selective pulses can be used in certain cases to distinguish between I_1 and I_2.

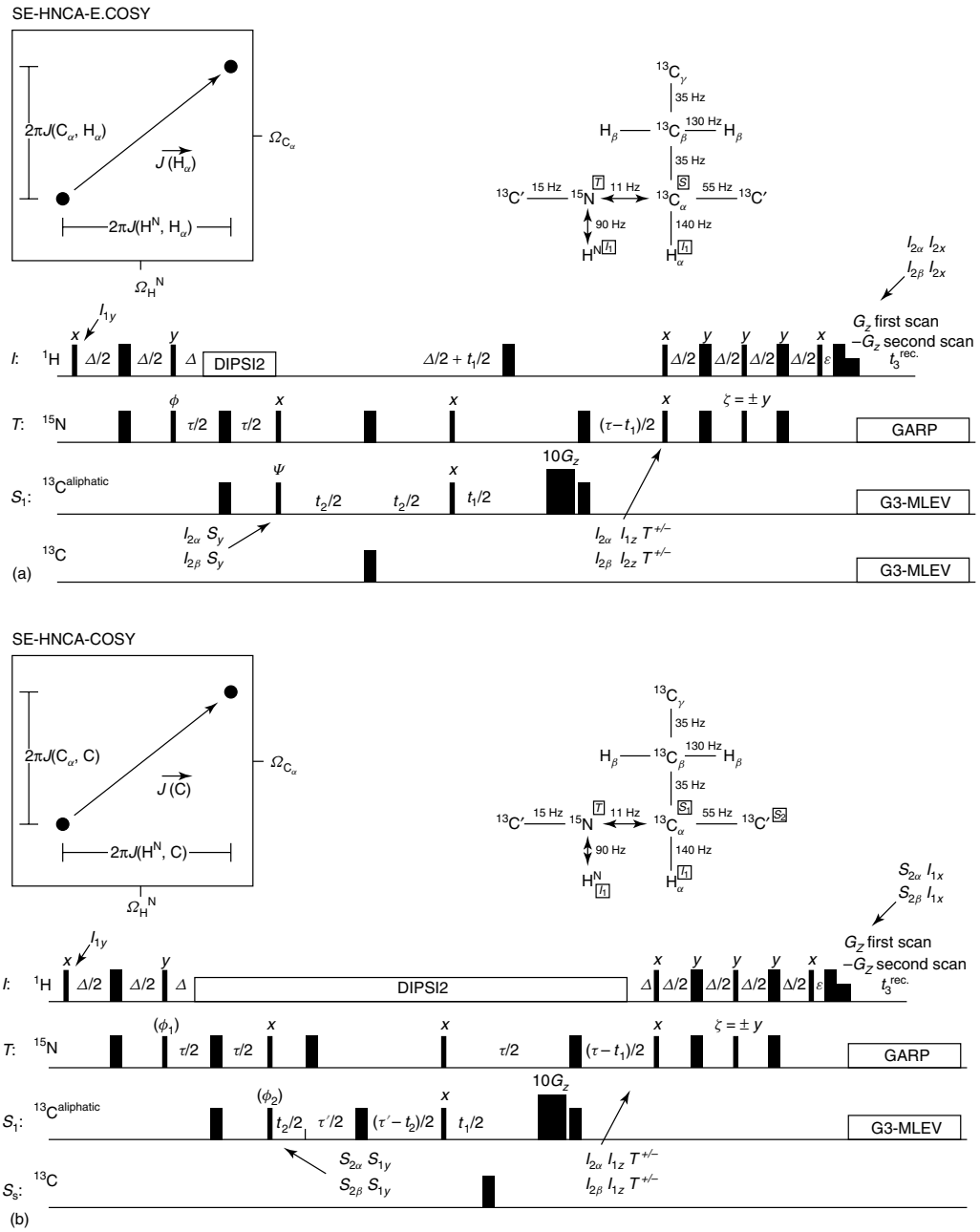

Figure 14.10. (a) HNCA-E.COSY with sensitivity enhancement and using a heteronuclear gradient echo to measure $^3J(H^N,H_\alpha)$ couplings. The parameters are: $\Delta = [2J(H^N,H_\alpha)]^{-1}$; $\tau = [2J(C_\alpha,N)]^{-1}$; $\tau' = [J(C_\alpha,C_\beta)]^{-1}$; $\epsilon = \tau_g$; $\phi = x, -x$; $\psi = x, x, -x, -x$; rec. $= x, -x, -x, x$. The coupling of interest is measured in the (ω_2,ω_3) plane of the three-dimensional experiment in cross peaks correlating C_α and H^N. The $^1J(C_\alpha,H_\alpha)$ coupling of 145 Hz serves as an associated coupling in ω_2. (b) SOFT-HNCA-COSY with sensitivity enhancement and using a heteronuclear gradient echo to measure $^3J(C',H^N)$ couplings. The parameters are the same as those in (a). The $^1J(C',C_\alpha)$ coupling of 55 Hz serves as an associated coupling in ω_2.

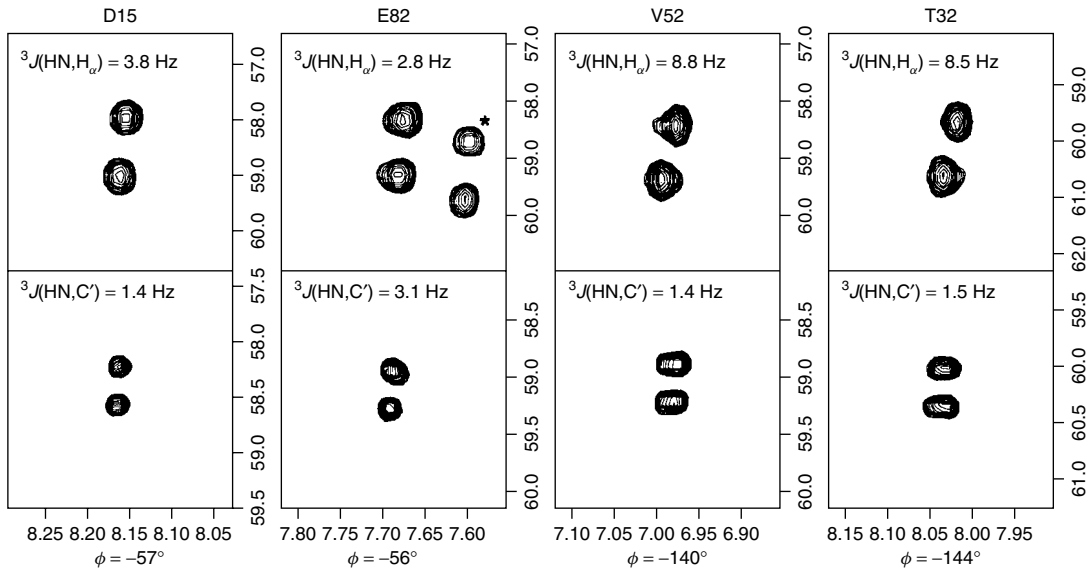

Figure 14.11. Cross peaks for Asp_{15}, Glu_{82}, Val_{52}, and Thr_{32}. Upper and lower traces show the C_α,H^N cross peaks from the SOFT-HNCA-E.COSY and the SOFT gradient enhanced HNCA-COSY. The $^3J(H^N,H_\alpha)$ and $^3J(C',H^N)$ coupling constants derived from the ω_3 splittings and the derived ϕ angles are indicated.

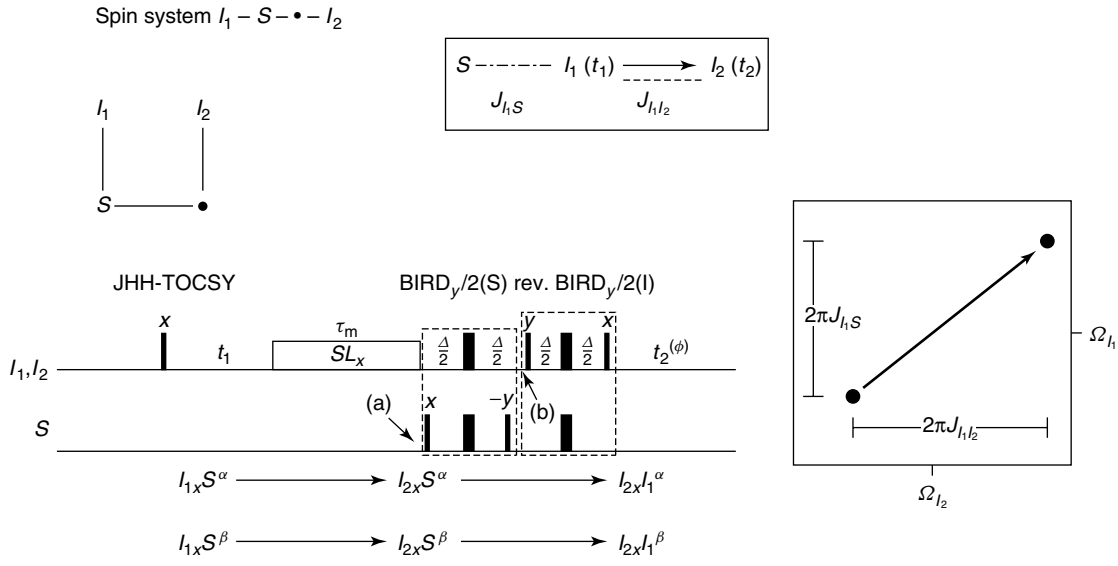

Figure 14.12. JHH-TOCSY for measuring $^nJ(I_1,I_2)$ couplings in a $I_1-S-\bullet-I_2$ spin system. The spin state of S in t_1 is transferred to the spin state of spin I_1 in t_1. Selection of a coherence transfer pathway by gradients,[17] although yielding a loss of a factor of $\sqrt{2}$ in signal-to-noise ratio compared with conventional HSQC experiments, is advantageous when measuring $^3J(H^N,H_\alpha)$ couplings in proteins, since the coupling is measured on the H_α resonance. Typical parameters are: $\Delta = [J(I_1,S)]^{-1}$; $\phi = x, -x$; rec. $= x, -x$. Scaling of the heteronuclear coupling could be implemented [see Figure 14.2(a)].

and SOFT-HNCA-COSY (see 14.3) obtained using gradient sensitivity enhanced correlation for the measuring of $^3J(H^N,H_\alpha)$ and $^3J(C',H^N)$ coupling constants, respectively. The resulting cross peaks are shown for four different cross peaks in ribonuclease T_1 in Figure 14.11. The combined analysis of these couplings leads to an unambiguous assignment of the ϕ-angle rotamer whenever only one rotamer around ϕ is populated.

Another implementation of the BIRD-filtering concept is the JHH-TOCSY developed by Willker and Leibfritz[55] (Figure 14.12). This experiment can be implemented in a spin system $I_1{-}S{-}\bullet{-}I_2$ with one kind of heterospin. The idea of this experiment is to use S as the passive spin during t_1. This encodes a frequency shift of $\pm\pi J(I_1,S)$ onto the I_1 multiplet for S^α and S^β, respectively. After the mixing (transfer from I_1 to I_2) the polarization of the S spin is completely transferred to polarization of the I_1 spin ($S^\alpha \rightarrow I_1^\alpha$; $S^\beta \rightarrow I_1^\beta$). Then, during t_2, a frequency shift of $\pm\pi J(I_1,I_2)$ is encoded for the two submultiplets that were displaced in ω_1 by $\pm\pi J(I_1,S)$. This transfer can be achieved by the sequence (Figure 14.12)

$$\underset{\text{(a)}}{I_{2x}(1/2 \pm S_z)} \rightarrow \underset{\text{(b)}}{I_{2x}(1/2 \pm 2I_{1z}S_z)} \rightarrow I_{2y}(1/2 \pm I_{1z}) = I_{2y}(1/2 \pm I_1^{\alpha/\beta}) \quad (14.2)$$

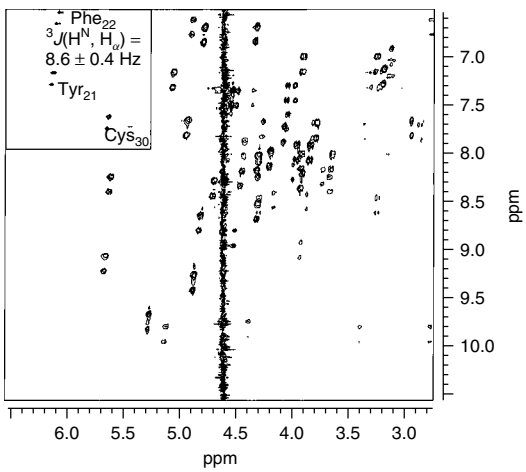

Figure 14.13. Two-dimensional plot of JHH-TOCSY applied to ^{15}N-enriched BPTI mutant[26] showing the excellent water suppression and the high sensitivity of the experiment.

Interestingly, this is the only experiment in this section that cannot be classified according an E.COSY triangle, since two different spins serve as passive spins in t_1 and t_2. The application of this experiment on a ^{15}N-enriched sample of a BPTI mutant using gradient coherence selection ensuring excellent water suppression is shown in Figure 14.13.[56] A $^3J(H^N,H_\alpha)$ coupling constant of 8.6 ± 0.4 Hz is found for Phe_{22}.

14.7 THE E.COSY EXPERIMENT FOR THE MEASUREMENT OF HOMONUCLEAR $^nJ(I_1,I_1)$ COUPLINGS IN AN $I_1{-}I_2{-}I_3$ SPIN SYSTEM AND $^nJ(I_1,I_2)$ COUPLINGS IN AN $I_1{-}S_1{-}\bullet{-}I_2$ SPIN SYSTEM

All the above mentioned methods impose special conditions on the spin system under study. The transfer between active spins, while not touching the passive spin, can be performed in homonuclear spin systems $I_1{-}I_2{-}I_3$ by a combination of experiments with different carefully chosen flip angle pulses in the E.COSY experiment (Figure 14.14).[1–3] An approximation to this procedure is the application of a small flip angle pulse in the P-E.COSY[2,57,58] experiment.

The transfer amplitudes of a polarization operator I_3^α or I_3^β are given by

$$I_3^\alpha \rightarrow I_3^\alpha \cos^2(\beta/2) + I_3^\beta \sin^2(\beta/2) \quad (14.3a)$$

$$I_3^\beta \rightarrow I_3^\beta \cos^2(\beta/2) + I_3^\alpha \sin^2(\beta/2) \quad (14.3b)$$

Thus choosing $\beta = 36^\circ$ gives a ratio for the undesired ($I_3^\alpha \rightarrow I_3^\beta$ and $I_3^\beta \rightarrow I_3^\alpha$) to the desired ($I_3^\alpha \rightarrow I_3^\alpha$ and $I_3^\beta \rightarrow I_3^\beta$) transfer of $\sin^2(\beta/2)/\cos^2(\beta/2) = \tan^2(\beta/2)$, which is about 10%. At the same time, polarization transfer between I_1 and I_2 ($2I_{1x}I_{2z} \rightarrow 2I_{1z}I_{2x}$) is achieved with a $\sin^2 \beta = 35\%$ efficiency compared with the value obtained for $\beta = 90^\circ$. Transfer between a heteronucleus S to I_1 is achieved with $\sin \beta = 59\%$ compared with $\beta = 90^\circ$. Due to the incomplete suppression of the nonconnected transitions, asymmetrical signal components that systematically shift the submultiplets together and lead to systematically smaller coupling constants are introduced.

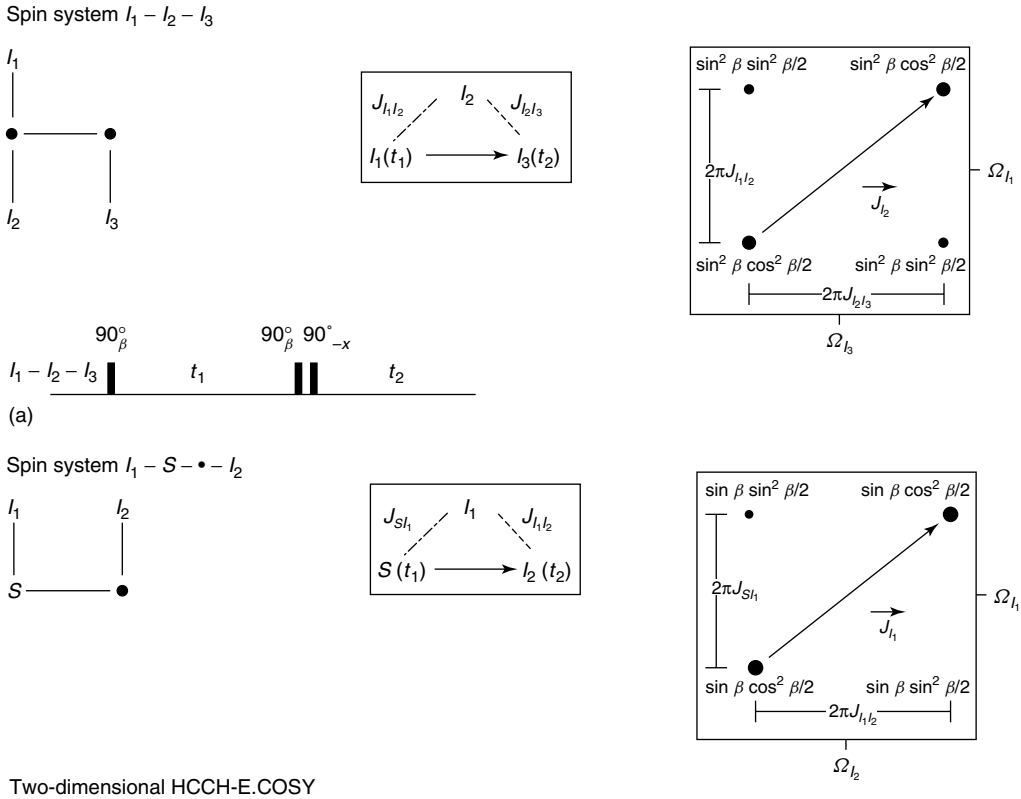

Figure 14.14. (a) The E.COSY experiment. In a homonuclear three-spin system, I_1 and I_3 are correlated by a $\beta \neq 90^\circ$ mixing pulse. The cross-peak intensities of connected and nonconnected transitions of I_2, depending on the mixing pulse β, are indicated. Preferentially, geminal $^2J(I_1,I_2)$ couplings serve as associated couplings in t_1. (b) The HCCH-E.COSY experiment. In a heteronuclear $I_1{-}S_1{-}\bullet{-}I_2$ spin system, S and I_2 are correlated by a $\beta_y(I) \neq 90^\circ$ mixing pulse implemented with phases according to the expansion: $\beta_y = 90^\circ_x \beta_z\ 90^\circ_{-x} = \beta_z\ 90^\circ_\beta\ 90^\circ_{-x}$. The cross-peak intensities of connected and nonconnected transitions of I_1, depending on the mixing pulse β, are indicated. The $^1J(S,I_1)$ coupling serves as the associated coupling in t_1. In the application to proteins, the $^1J(C',C_\alpha)$ coupling should be refocused in t_1, as should long-range $^3J(C',H_\beta)$ coupling in t_1. The parameters are: $\Delta = [2J(C_\alpha,H_\alpha)]^{-1}$; $\tau = [2J(C_\alpha,C_\beta)]^{-1}$; $\tau' = [4J(C_\alpha,C_\beta)]^{-1}$; $\Delta' = [2J(C_\alpha,H_\alpha)]^{-1}$; $\phi = x, -x$; $\psi = x, x, -x, -x$; rec. $= x, -x, -x, x$. The same pulse sequence can be used to measure J(C,H) couplings in oligonucleotides when replacing P for C′. A source of systematically smaller couplings is the evolution of chemical shift of the two rows displaced in ω_2 by $J(I_1,I_2)$. The acquired phase difference $\Delta\phi$ depends on the size of the coupling constants of interest and is given for a refocusing delay Δ: $\Delta\phi = J(\text{H,H}) \cdot \Delta \cdot 360^\circ$. This phase difference can easily be corrected for by different phasing of the two extracted rows.

Dispersive diagonal peak contributions can be suppressed in the P-E.COSY experiment by subtraction of a second experiment with $\beta = 0^\circ$.

The E.COSY procedure relies on a linear combination of different flip angles β that are chosen so as to suppress completely the undesired nonconnected transitions. The deduction of flip angles and weights depends upon the spin system under study. For more details, the interested reader is referred to the paper by Griesinger *et al.*[2]

Figure 14.15 shows the Pro_8 β_2/γ_2 cross peak in antamanide, and the corresponding displacement vectors in this CH_2–CH_2 fragment.[3] E.COSY and P-E.COSY sequences have been successfully applied to peptides and proteins and to oligonucleotides[116–127] to obtain local conformational information. For completeness, a gradient selected E.COSY experiment based on the linear combination of multiple quantum filtered COSY spectra has been published.[128] The sensitivity of such an experiment is, however, considerably reduced compared with the "nongradient" versions of E.COSY or P-E.COSY.

For ^{13}C-labeled proteins the HCCH-E.COSY experiment [Figure 14.14(b)] can be applied to obtain proton–proton coupling constants in $H^{13}C$–$^{13}CH_m$ fragments (where m is the number of protons attached to the carbon atom). In this case only small flip angle pulses[27,129] or selective pulses[130] can be applied in order to fulfill the E.COSY condition, leaving one of the protons untouched in the final C → H transfer. Other implementations using TOCSY for the C → C transfer have been proposed by Emerson and Montelione.[131,132] The determination of H,H coupling constants in $H_k{}^{13}C$–$^{13}CH_m$ moieties is described in the paper by Eggenberger *et al.*[27]

The number of relevant spins for the C → H spin transfer is either two (I_1–S_1–•–I_2) or three (I_1,I_1'–S_1–•–I_2). Coupling constants to protons of methyl groups (I_1,I_1',I_1''–S_1–•–I_2) are normally not of great interest, due to conformational averaging. The transfer amplitude for a C → H INEPT-type transfer is thus given by $\sin\beta\cos^2(\beta/2)$ for the I_1–S_1–•–I_2 spin system and $\sin\beta\cos\beta\cos^2(\beta/2)$ for the I_1,I_1'–S_1–•–I_2 spin system. For $\beta_1 = 44.4$ with a weight of 6 and $\beta_2 = 135.6$ with a weight of 1 for the I_1–S_1–•–I_2 and −1 for the I_1,I_1'–S_1–•–I_2 spin systems, the undesired components vanish completely.[133]

The application of such an HCCH-E.COSY sequence applied to ^{13}C-labeled 5′-GMP (guanosine 5′-monophosphate)[133] is shown in Figure 14.16. The conformational analysis reveals an N/S-conformer equilibrium of 70:30.

A further sensitivity improvement of the HCCH-E.COSY experiment[134] is provided by a "DEPT transfer" for the last C → H transfer, as demonstrated in Figure 14.17. If only CH groups are detected, no gain is obtained. The gain in sensitivity of the "DEPT" version compared with the "INEPT" [Figure 14.14(b)] version for CH, CH_2, and CH_3 groups, provided the same flip angle β is used for the proton pulse in each case, is given in Table 14.1.

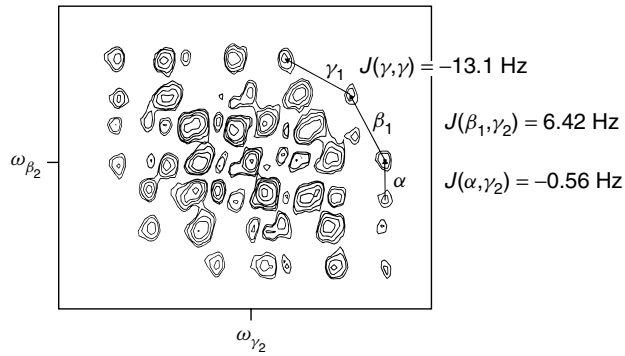

Figure 14.15. $H_{\beta 2} \rightarrow H_{\gamma 2}$ cross peak multiplet of Pro_8 in the 300 MHz ^{1}H spectrum of antamanide. The displacement vectors due to the three passive spins H_α, $H_{\beta 1}$, and $H_{\gamma 1}$ are clearly visible. All three vectors point from lower right to upper left. Assuming a negative sign for the aliphatic ^2J(H,H) coupling constants, the vicinal coupling $J(H_{\beta 1},H_{\gamma 2})$ is found to be positive and, due to the positive coupling constant between H_α and $H_{\beta 2}$ found in another cross peak, the $^4J(\alpha_1,\gamma_2)$ coupling is found to be negative.[3]

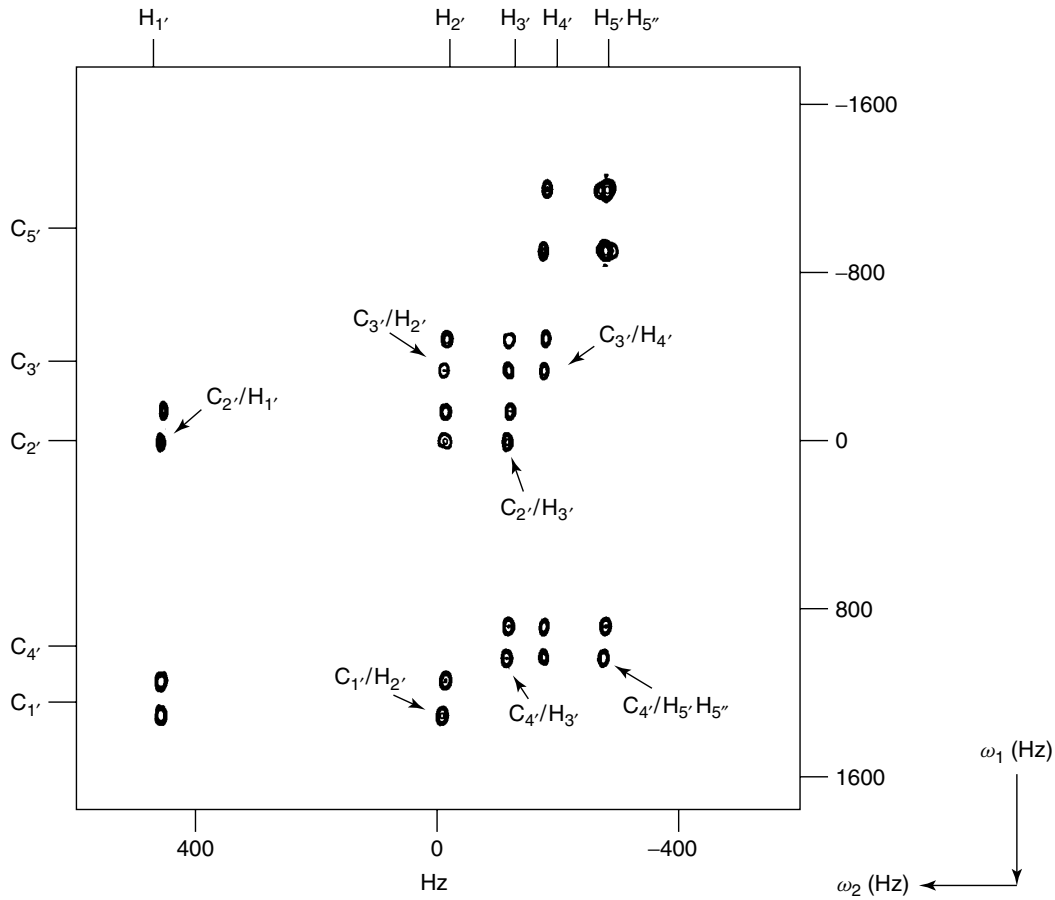

Figure 14.16. A 400 MHz HCCH-E.COSY spectrum with flip angle β for $^{13}C,^{15}N$ labeled 5′-GMP. The doublet structure in the two frequency dimensions is clearly visible.

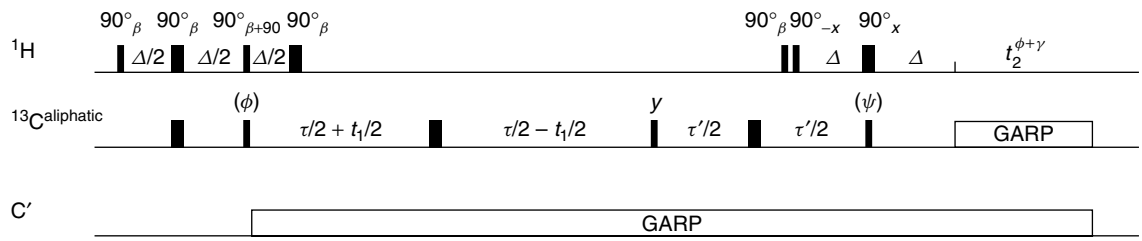

Figure 14.17. HCCH-E.COSY with a final 'DEPT' C7 → H transfer. The flip angle β is chosen such that the nonconnected transitions are suppressed. Alternatively, two experiments with $\beta = 44.4^\circ$ and 135.6° and weights of 6 and 1, respectively, are combined, as described for the 'INEPT' version.

Table 14.1. Sensitivity gain provided by a 'DEPT transfer'

	^{13}CH	$^{13}CH_2$	$^{13}CH_3$
S(DEPT)/S(INEPT)[a]	$1/\sin \pi J(C,H)\Delta'$	$\cos\theta/[\sin \pi J(C,H)\Delta' \cos \pi J(C,H)\Delta']$	$\cos^2\theta/[\sin \pi J(C,H)\Delta' \cos^2 \pi J(C,H)\Delta']$
$\Delta' = 1/2J(CH)$	1	–	–
$\Delta' = 1/4J(CH)$	1.41	1.62	1.85
$\Delta' = 0/2J(CH)$	1.7	1.7	1.7

[a] Δ' refers to the refocusing delay of the 'INEPT' version.

REFERENCES

1. C. Griesinger, O. W. Sørensen, and R. R. Ernst, *J. Am. Chem. Soc.*, 1985, **107**, 6394.
2. C. Griesinger, O. W. Sørensen, and R. R. Ernst, *J. Chem. Phys.*, 1986, **85**, 6837.
3. C. Griesinger, O. W. Sørensen, and R. R. Ernst, *J. Magn. Reson.*, 1987, **75**, 474.
4. G. S. Harbison, *J. Am. Chem. Soc.*, 1993, **115**, 3026.
5. T. J. Norwood, *J. Magn. Reson., Ser. A*, 1993, **101**, 109.
6. T. J. Norwood and K. Jones, *J. Magn. Reson., Ser. A*, 1993, **104**, 106.
7. R. E. London, *J. Magn. Reson.*, 1990, **86**, 410.
8. P. Schmidt, H. Schwalbe, and C. Griesinger, unpublished results.
9. G. Montelione and G. Wagner, *J. Am. Chem. Soc.*, 1989, **111**, 5474.
10. G. Montelione and G. Wagner, *J. Magn. Reson.*, 1990, **87**, 183.
11. A. Bax and R. Freeman, *J. Magn. Reson.*, 1981, **45**, 177.
12. M. Kurz, P. Schmieder, and H. Kessler, *Angew. Chem.*, 1991, **103**, 1341.
13. P. Schmieder, M. Kurz, and H. Kessler, *J. Biomol. NMR*, 1991, **1**, 403.
14. A. S. Edison, W. M. Westler, and J. L. Markley, *J. Magn. Reson.*, 1991, **92**, 434.
15. E. R. P. Zuiderweg and S. W. Fesik, *J. Magn. Reson.*, 1991, **93**, 653.
16. D. F. Mierke, P. Schmieder, P. Karuso, and H. Kessler, *Helv. Chim. Acta*, 1991, **74**, 1027.
17. P. Schmieder and H. Kessler, *Biopolymers*, 1992, **32**, 435.
18. M. Sattler, H. Schwalbe, and C. Griesinger, *J. Am. Chem. Soc.*, 1992, **114**, 1126.
19. J. Schleucher, B. Schwörer, C. Zirngibl, U. Koch, W. Weber, E. Egert, R. K. Thauer, and C. Griesinger, *FEBS Lett.*, 1992, **314**, 440.
20. L. Poppe, W. S. York, and H. van Halbeek, *J. Biomol. NMR*, 1993, **3**, 81.
21. J. V. Hines, G. Varani, S. M. Landry, and I. Tinoco, *J. Am. Chem. Soc.*, 1993, **115**, 11 002.
22. U. Wollborn, W. Willker, and D. Leibfritz, *J. Magn. Reson., Ser. A*, 1993, **103**, 86.
23. G. T. Montelione, M. E. Winkler, P. Rauenbühler, and G. Wagner, *J. Magn. Reson.*, 1989, **82**, 198.
24. P. Schmieder, J. H. Ippel, H. van den Elst, G. H. van der Marel, J. H. van Boom, C. Altona, and H. Kessler, *Nucleic Acids Res.*, 1992, **20**, 4747.
25. E. Worgötter, G. Wagner, M. Vasak, J. H. R. Kagi, and K. Wüthrich, *J. Am. Chem. Soc.*, 1988, **110**, 2388.
26. I. D. Rae, J. A. Weigold, R. H. Contreras, and G. Yamamoto, *Magn. Reson. Chem.*, 1992, **30**, 1047.
27. U. Eggenberger, Y. Karimi-Nejad, H. Thüring, H. Rüterjans, and C. Griesinger, *J. Biomol. NMR*, 1992, **2**, 583.
28. M. McCoy and L. Müller, *J. Am. Chem. Soc.*, 1992, **114**, 2108.
29. M. McCoy and L. Müller, *J. Magn. Reson.*, 1992, **98**, 674.
30. M. McCoy and L. Müller, *J. Magn. Reson.*, 1992, **99**, 18.
31. U. Eggenberger, P. Schmidt, M. Sattler, S. J. Glaser, and C. Griesinger, *J. Magn. Reson.*, 1992, **100**, 604.
32. M. McCoy and L. Müller, *J. Magn. Reson., Ser. A*, 1993, **101**, 122.
33. M. D. Sørensen, S. M. Kristensen, J. J. Led, and O. W. Sørensen, *J. Magn. Reson. Ser. A*, 1993, **103**, 364.

34. R. Brüschweiler, J. C. Madsen, C. Griesinger, O. W. Sørensen, and R. R. Ernst, *J. Magn. Reson.*, 1987, **73**, 380.
35. P. Berthault, H. Desvaux, and B. Perly, *Magn. Reson. Chem.*, 1993, **31**, 259.
36. L. Emsley, T. J. Dwyer, H. P. Spielmann, and D. E. Wemmer, *J. Am. Chem. Soc.*, 1993, **115**, 7765.
37. R. Konrat, G. Zieger, and H. Sterk, *Chem. Phys. Lett.*, 1993, **212**, 78.
38. L. Emsley and G. Bodenhausen, *J. Magn. Reson.*, 1989, **82**, 211.
39. L. Emsley and G. Bodenhausen, *Chem. Phys. Lett.*, 1990, **165**, 469.
40. H. Geen and R. Freeman, *J. Magn. Reson.*, 1991, **93**, 93.
41. G. W. Vuister and A. Bax, *J. Biomol. NMR*, 1992, **2**, 401.
42. R. Weisemann, H. Rüterjans, H. Schwalbe, J. Schleucher, W. Bermel, and C. Griesinger, *J. Biomol. NMR*, 1994, **4**, 231.
43. S. Seip, J. Balbach, and H. Kessler, *J. Magn. Reson.*, 1994, **B104**, 172.
44. H. Kessler, U. Anders, and G. Gemmecker, *J. Magn. Reson.*, 1988, **78**, 382.
45. G. Zhu and A. Bax, *J. Magn. Reson.*, 1992, **98**, 192.
46. G. Zhu and A. Bax, *J. Magn. Reson.*, 1990, **90**, 405.
47. H. Schwalbe, A. Rexroth, U. Eggenberger, T. Geppert, and C. Griesinger, *J. Am. Chem. Soc.*, 1993, **114**, 7878.
48. J. R. Garbow, D. P. Weitekamp, and A. Pines, *Chem. Phys. Lett.*, 1982, **93**, 504.
49. O. W. Sørensen, *J. Magn. Reson.*, 1990, **90**, 433.
50. J. C. Madsen, O. W. Sørensen, P. Sørensen, and F. M. Poulsen, *J. Biomol. NMR*, 1993, **3**, 239.
51. S. Seip, J. Balbach, and H. Kessler, *Angew. Chem., Int. Ed. Engl.*, 1992, **31**, 1609.
52. G. Wagner, P. Schmieder, and V. Thanabal, *J. Magn. Reson.*, 1991, **93**, 436.
53. S. D. Emerson and G. T. Montelione, *J. Magn. Reson.*, 1992, **99**, 413.
54. M. Gorlach, M. Wittekind, B. T. Farmer, L. E. Kay, and L. Müller, *J. Magn. Reson., Ser. B*, 1993, **101**, 194.
55. W. Willker and D. Leibfritz, *J. Magn. Reson.*, 1992, **99**, 421.
56. H. Schwalbe, H. Oschkinat, W. Bermel, P. Schmitt, and C. Griesinger, unpublished data.
57. L. Müller, *J. Magn. Reson.*, 1987, **72**, 191.
58. A. Bax and D. Marion, *J. Magn. Reson.*, 1988, **80**, 528.
59. H. Kessler, G. Gemmecker, A. Haupt, M. Klein, K. Wagner, and M. Will, *Tetrahedron*, 1988, **44**, 745.
60. P. C. Driscoll, G. M. Clore, and A. M. Gronenborn, *FEBS Lett.*, 1989, **243**, 223.
61. P. C. Driscoll, G. M. Clore, L. Beress, and A. M. Gronenborn, *Biochemistry*, 1989, **28**, 2178.
62. H. Kessler, A. Müller, and K. H. Pook, *Liebigs Ann. Chem.*, 1989, **9**, 903.
63. H. Kessler, J. W. Bats, K. Wagner, and M. Will, *Biopolymers*, 1989, **28**, 385.
64. P. J. M. Folkers, G. M. Clore, P. C. Driscoll, J. Dodt, S. Kohler, and A. M. Gronenborn, *Biochemistry*, 1989, **28**, 2601.
65. H. Kessler, M. Will, J. Antel, H. Beck, and G. M. Sheldrick, *Helv. Chim. Acta*, 1989, **72**, 530.
66. H. Haruyama, Y. Q. Qian, and K. Wüthrich, *Biochemistry*, 1989, **28**, **4301**, 4312.
67. C. Redfield and C. M. Dobson, *Biochemistry*, 1990, **29**, 7201.
68. H. Kessler, S. Mronga, M. Will, and U. Schmidt, *Helv. Chim. Acta*, 1990, **73**, 25.
69. M. Billeter, Y. Qian, G. Otting, M. Müller, W. J. Gehring, and K. Wüthrich, *J. Mol. Biol.*, 1990, **214**, 183.
70. H. Kessler, U. Anders, and M. Schudok, *J. Am. Chem. Soc.*, 1990, **112**, 5908.
71. B. A. Messerle, A. Schaffer, M. Vasak, J. H. R. Kagi, and K. Wüthrich, *J. Mol. Biol.*, 1990, **214**, 765.
72. P. Karuso, H. Kessler, and D. F. Mierke, *J. Am. Chem. Soc.*, 1990, **112**, 9434.
73. Y. M. Kim and J. H. Prestegard, *Proteins Struct. Func. Genet.*, 1990, **8**, 377.
74. J. Habazettl, C. Cieslar, H. Oschkinat, and T. A. Holak, *FEBS Lett.*, 1990, **268**, 141.
75. L. J. Smith, M. J. Sutcliffe, C. Redfield, and C. M. Dobson, *Biochemistry*, 1991, **30**, 986.
76. J. M. Moore, C. A. Lepre, G. P. Gippert, W. J. Chazin, D. A. Case, and P. E. Wright, *J. Mol. Biol.*, 1991, **221**, 533.

77. J. M. Schmidt, O. Ohlenschläger, H. Rüterjans, Z. Grzanka, E. Kojro, I. Pavo, and F. Fahrenholz, *Eur. J. Biochem.*, 1991, **201**, 355.
78. H. Kessler, S. Mronga, G. Müller, L. Moroder, and R. Huber, *Biopolymers*, 1991, **31**, 1189.
79. A. L. Breeze, T. S. Harvey, R. Bazzo, and I. D. Campbell, *Biochemistry*, 1991, **30**, 575.
80. H. Kessler, H. Matter, G. Gemmecker, A. Kling, and M. Kottenhahn, *J. Am. Chem. Soc.*, 1991, **113**, 7550.
81. K. H. Ott, S. Becker, R. D. Gordon, and H. Rüterjans, *FEBS Lett.*, 1991, **278**, 160.
82. C. Abeygunawardana, C. A. Bush, and J. O. Cisar, *Biochemistry*, 1991, **30**, 8568.
83. P. Sodano, T. H. Xia, J. H. Bushweller, O. Bjornberg, A. Holmgren, M. Billeter, and K. Wüthrich, *J. Mol. Biol.*, 1991, **221**, 1311.
84. D. Seebach, S. Y. Ko, H. Kessler, M. Köck, M. Reggelin, P. Schmieder, M. D. Walkinshaw, J. J. Bölsterli, and D. Bevec, *Helv. Chim. Acta*, 1991, **74**, 1953.
85. X. Li, M. J. Sutcliffe, T. W. Schwartz, and C. M. Dobson, *Biochemistry*, 1992, **31**, 1245.
86. U. Hommel, T. S. Harvey, P. C. Driscoll, and I. D. Campbell, *J. Mol. Biol.*, 1992, **227**, 271.
87. J. Freund, A. Kapurniotu, T. A. Holak, M. Lenfant, and W. Voelter, *Z. Naturforsch., B*, 1992, **47**, 1324.
88. D. Neri, M. Billeter, and K. Wüthrich, *J. Mol. Biol.*, 1992, **223**, 743.
89. H. Kessler, H. Matter, G. Gemmecker, M. Kottenhahn, and J. W. Bats, *J. Am. Chem. Soc.*, 1992, **114**, 4805.
90. G. T. Montelione, K. Wüthrich, A. W. Burgess, E. C. Nice, G. Wagner, K. D. Gibson, and H. A. Scheraga, *Biochemistry*, 1992, **31**, 236.
91. M. Köck, H. Kessler, D. Seebach, and A. Thaler, *J. Am. Chem. Soc.*, 1992, **114**, 2676.
92. P. J. Kraulis, A. R. C. Raine, P. L. Gadhavi, and E. D. Laue, *Nature*, 1992, **356**, 448.
93. M. Reggelin, H. Hoffmann, M. Köck, and D. F. Mierke, *J. Am. Chem. Soc.*, 1992, **114**, 3272.
94. T. H. Xia, J. H. Bushweller, P. Sodano, M. Billeter, O. Bjornberg, A. Holmgren, and K. Wüthrich, *Protein Sci.*, 1992, **1**, 310.
95. B. A. Messerle, A. Schaffer, M. Vasak, J. H. R. Kagi, and K. Wüthrich, *J. Mol. Biol.*, 1992, **225**, 433.
96. J. Saulitis, D. F. Mierke, G. Byk, C. Gilon, and H. Kessler, *J. Am. Chem. Soc.*, 1992, **114**, 4818.
97. H. Kessler, A. Geyer, H. Matter, and M. Köck, *Int. J. Pept. Protein Res.*, 1992, **40**, 25.
98. K. D. Berndt, P. Guntert, L. P. M. Orbons, and K. Wüthrich, *J. Mol. Biol.*, 1992, **227**, 757.
99. K. Wakamatsu, D. Kohda, H. Hatanaka, J. M. Lancelin, Y. Ishida, M. Oya, H. Nakamura, F. Inagaki, and K. Sato, *Biochemistry*, 1992, **31**, 12. 577.
100. T. Szyperski, P. Guntert, S. R. Stone, and K. Wüthrich, *J. Mol. Biol.*, 1992, **228**, 1193.
101. M. Gurrath, G. Müller, H. Kessler, M. Aumailley, and R. Timpl, *Eur. J. Biochem.*, 1992, **210**, 911.
102. N. Fusetani, K. Shimoda, and S. Matsunaga, *J. Am. Chem. Soc.*, 1993, **115**, 3977.
103. A. Schnuchel, R. Wiltschek, M. Czisch, M. Herrler, G. Willimsky, P. Graumann, M. A. Marahiel, and T. A. Holak, *Nature*, 1993, **364**, 169.
104. R. K. Konat, D. F. Mierke, H. Kessler, B. Kutscher, M. Bernd, and R. Voegeli, *Helv. Chim. Acta*, 1993, **76**, 1649.
105. S. Mronga, G. Müller, J. Fischer, and F. Riddell, *J. Am. Chem. Soc.*, 1993, **115**, 8414.
106. J. Kordel, N. J. Skelton, M. Arke, and W. J. Chazin, *J. Mol. Biol.*, 1993, **231**, 711.
107. L. R. Brown, S. Mronga, R. A. Bradshaw, C. Ortenzi, P. Luporini, and K. Wüthrich, *J. Mol. Biol.*, 1993, **231**, 800.
108. Y. Blancuzzi, A. Padilla, J. Parello, and A. Cave, *Biochemistry*, 1993, **32**, 1302.
109. H. Kessler, R. Haessner, and W. Schuler, *Helv. Chim. Acta*, 1993, **76**, 117.
110. Y. N. Kalia, S. M. Brocklehurst, D. S. Hipps, E. Appella, K. Sakaguchi, and R. N. Perham, *J. Mol. Biol.*, 1993, **230**, 323.
111. W. Antuch, K. D. Berndt, M. A. Chavez, J. Delfin, and K. Wüthrich, *Eur. J. Biochem.*, 1993, **212**, 675.
112. J. F. O′Connell, P. E. Bougis, and K. Wüthrich, *Eur. J. Biochem.*, 1993, **213**, 891.
113. J. H. Davis, E. K. Bradley, G. P. Miljanich, L. Nadasdi, J. Ramachandran, and V. J. Basus, *Biochemistry*, 1993, **32**, 7396.
114. K. Bartik, C. M. Dobson, and C. Redfield, *Eur. J. Biochem.*, 1993, **215**, 255.
115. K. D. Berndt, P. Guntert, and K. Wüthrich, *J. Mol. Biol.*, 1993, **234**, 735.
116. A. Bax and L. Lerner, *J. Magn. Reson.*, 1988, **79**, 429.

117. U. Schmitz, G. Zon, and T. L. James, *Biochemistry*, 1990, **29**, 2357.

118. A. Foldesi, P. Agback, C. Glemarec, and J. Chattopadhyaya, *Tetrahedron*, 1991, **47**, 7135.

119. W. J. Chazin, M. Rance, A. Chollet, and W. Leupin, *Nucleic Acids Res.*, 1991, **19**, 5507.

120. S. M. Chen, W. Leupin, and W. J. Chazin, *Int. J. Biol. Macromol.*, 1992, **14**, 57.

121. S. M. Chen, W. Leupin, M. Rance, and W. J. Chazin, *Biochemistry*, 1992, **31**, 4406.

122. J. W. Cheng, S. H. Chou, M. Salazar, and B. R. Reid, *J. Mol. Biol.*, 1992, **228**, 118.

123. S. H. Chou, J. W. Cheng, and B. R. Reid, *J. Mol. Biol.*, 1992, **228**, 138.

124. S. G. Kim, L. J. Lin, and B. R. Reid, *Biochemistry*, 1992, **31**, 3564.

125. S. G. Kim and B. R. Reid, *Biochemistry*, 1992, **31**, 12. 103.

126. M. Salazar, J. J. Champoux, and B. R. Reid, *Biochemistry*, 1993, **32**, 739.

127. M. Salazar, O. Y. Fedoroff, J. M. Miller, N. S. Ribeiro, and B. R. Reid, *Biochemistry*, 1993, **32**, 4207.

128. W. Willker, D. Leibfritz, R. Kerssebaum, and J. Lohman, *J. Magn. Reson., Ser. A*, 1993, **102**, 348.

129. C. Griesinger and U. Eggenberger, *J. Magn. Reson.*, 1992, **97**, 426.

130. G. Gemmecker and S. W. Fesik, *J. Magn. Reson.*, 1991, **95**, 208.

131. S. D. Emerson and G. T. Montelione, *J. Magn. Reson.*, 1992, **99**, 413.

132. S. D. Emerson and G. T. Montelione, *J. Am. Chem. Soc.*, 1992, **114**, 354.

133. H. Schwalbe, G. C. King, R. Wechselberger, W. Bermel, and C. Griesinger, *J. Biomol. NMR*, 1994, **4**, 631.

134. H. B. Olsen, S. Ludvigsen, and O. W. Sørensen, *J. Magn. Reson., Ser. A*, 1993, **104**, 226.